

Phonon-assisted transitions and optical gain in indirect semiconductors

Sebastian Imhof* and Angela Thränhardt

Institut für Physik, Technische Universität Chemnitz, 09107 Chemnitz, Germany

(Received 10 May 2010; revised manuscript received 29 June 2010; published 3 August 2010)

Microscopic semiconductor theory is applied to an indirect Si-type semiconductor quantum well system. We discuss the absorption and stimulated emission of light accompanied by the creation or annihilation of phonons. We find strong differences to the optical properties of conventional direct semiconductors, including an asymmetric behavior where the maximum gain strongly exceeds the low-density absorption.

DOI: [10.1103/PhysRevB.82.085303](https://doi.org/10.1103/PhysRevB.82.085303)

PACS number(s): 78.20.Bh, 78.66.Db, 63.20.kd, 78.67.De

I. INTRODUCTION

Silicon-based photonics is one of the most active research areas of our time, there being various approaches to the integration of optical devices on a silicon chip: (1) The quest for a direct III-V-semiconductor that can be grown on silicon, i.e., where the mismatch in lattice constants is sufficiently small or nonexistent. Recently, (GaIn)(NAsP) has been identified as an appropriate candidate and is investigated intensively at the moment.¹ (2) The design of silicon-based optical devices. This is extremely complicated because silicon as an indirect semiconductor does not readily emit light. Yet there has been a variety of approaches²⁻⁴ including the use of porous silicon⁵ or SiO₂/Si superlattices.^{6,7}

Silicon has long been considered unsuitable for optical applications because of its indirect character and weakness of optical transitions.⁸ More recent measurements of photoluminescence quantum efficiencies of up to 10.2% of Silicon wafers, however, have readdressed the question and left it wide open.⁹ These results shift silicon into the focus of semiconductor theory. So far, its optical properties have only been treated in simple one-particle models. Rate models were used to calculate the gain coefficient in indirect materials.^{10,11} Trupke *et al.* give an estimate of the gain coefficient using a two-level system and propose that the optical properties of indirect semiconductors are fundamentally different from the well-known characteristics of direct materials.¹² Specifically, the gain of indirect transitions can be orders of magnitude higher than their positive absorption coefficient.

Haug and Koch have considered exciton-phonon processes in material systems such as CdS and ZnO and have in this way included indirect phonon-assisted absorption and gain in their excitonic model.^{13,14} The calculation, however, is not directly transferable to silicon-type structures because it requires the exciton energy to be large compared to the phonon energy, which is not the case in silicon ($E_B \approx 14$ meV and $\hbar\Omega_{LO,\Gamma} \approx 52$ meV) and germanium ($E_B = 3-4$ meV and $\hbar\Omega_{LO,\Gamma} \approx 37$ meV).¹⁵

It is well-known that many body effects fundamentally change the shape and properties of optical transitions.¹⁶ Semiconductor theory has advanced to a high precision where we even reach predictive power and are able to use simulations in material and device development.¹⁷⁻¹⁹ In quantum well systems one can often neglect memory effects of the electron-phonon scattering whereas in quantum-dots non-Markovian effects have been a topic of intense discus-

sion recently.²⁰⁻²² In the calculation of absorption and gain in an indirect semiconductor the Markov-approximation is not compatible with the structure of the equations of motion (see Sec. II).

In this paper, we extend microscopic theory to indirect Si-type semiconductors. Compared to the direct system, e.g., GaAs, modeling of optical transitions becomes more complex due to additional particles, generally phonons, being involved. We apply the equation-of-motion approach to an indirect semiconductor quantum well structure in order to model the optical properties including the Coulomb interaction between carriers.

II. THEORY

One intention of this publication is to investigate whether the propositions made by Trupke and coauthors,¹² namely, that the gain of indirect transitions can be orders of magnitude higher than their absorption, still hold when including many-particle interaction. We therefore choose our parameters in analogy to the ones used in Ref. 12.

We assume a quasi-two-dimensional model system which allows a discussion of the fundamental properties of the indirect interband transitions. As usual, we assume a three-dimensional phonon system because of the similarity of the elastic constants in the well and barrier materials.²³

To derive the equations of motion, we first need to specify the system Hamiltonian. The operators $a_{\mu,\mathbf{k}}^\dagger$ ($a_{\mu,\mathbf{k}}$) denote the creation (annihilation) of electrons in the μ th subband with wave number \mathbf{k} . The bosonic operators are represented by $b_{\alpha,\mathbf{q}}^\dagger$ ($b_{\alpha,\mathbf{q}}$) and denote the creation (annihilation) of phonons, where α denotes the phonon-branch.

The system is described by the Hamiltonian

$$H = H_{sp} + H_C + H_{ph-sp} + H_{e-ph} + H_L, \quad (1)$$

where

$$H_{sp} = \sum_{\mathbf{k},\mu} E_{\mu,\mathbf{k}} a_{\mu,\mathbf{k}}^\dagger a_{\mu,\mathbf{k}} \quad (2)$$

is the kinetic energy with the single-particle energies $E_{\mu,\mathbf{k}}$. These energies are given by the band structure which is shown in Fig. 1(a) and will be discussed in detail in Sec. III

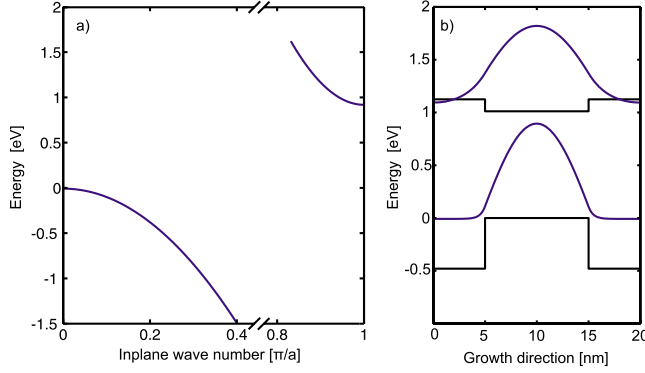


FIG. 1. (Color online) (a) Band structure of the two band model assuming a complete separation of electrons and holes in momentum space for in plane wave numbers k . (b) Confinement potentials and wave functions of the conduction band at the boundary of the first Brillouin zone and of the valence band at the Γ -Point in growth direction.

$$H_C = \frac{1}{2} \sum_{\substack{\mathbf{k}, \mathbf{k}', \mathbf{q} \neq 0 \\ \mu, \nu}} \gamma_{\mu, \nu}^{\mathbf{k}, \mathbf{k}'}(\mathbf{q}) V_q a_{\mu, \mathbf{k}+\mathbf{q}}^\dagger a_{\nu, \mathbf{k}'-\mathbf{q}}^\dagger a_{\nu, \mathbf{k}'} a_{\mu, \mathbf{k}} \quad (3)$$

is the Coulomb interaction with the two-dimensional Coulomb-matrix element

$$V_q^{2D} = \frac{1}{4\pi\epsilon_0 L^2} \frac{1}{q} \quad (4)$$

and the confinement factor

$$\gamma_{\mu, \nu}^{\mathbf{k}, \mathbf{k}'}(\mathbf{q}) = \frac{1}{2\pi} \int dz_1 \int dz_2 \times \zeta_{\mu, \mathbf{k}+\mathbf{q}}(z_1) \zeta_{\nu, \mathbf{k}'-\mathbf{q}}(z_2) e^{-q|z_2-z_1|} \zeta_{\nu, \mathbf{k}}(z_1) \zeta_{\mu, \mathbf{k}'}(z_2), \quad (5)$$

where $\zeta_{\nu, \mathbf{k}}(z)$ are the electron wave functions. These are shown in Fig. 1(b), where we assume a carrier confinement of valence-band and conduction-band electrons in their respective band minima, i.e., conduction-band electrons and valence-band electrons are confined at the end of the first Brillouin zone and at the Γ point, respectively.

$$H_L = \sum_{\mathbf{k}, \mu, \nu} \mathcal{E}(t) a_{\mu, \mathbf{k}}^\dagger a_{\nu, \mathbf{k}} d_{\mu\nu}(\mathbf{k}) \quad (6)$$

is the light-matter interaction with the classical light-field $\mathcal{E}(t)$ and the dipole matrix-element $d_{\mu\nu}(\mathbf{k})$,

$$H_{ph-sp} = \sum_{\alpha, \mathbf{q}} \hbar \Omega_\alpha(\mathbf{q}) b_{\alpha, \mathbf{q}}^\dagger b_{\alpha, \mathbf{q}} \quad (7)$$

is the kinetic energy of the phonons with the energy $\hbar \Omega_\alpha(\mathbf{q})$, and

$$H_{e-ph} = \sum_{\mu, \alpha, \mathbf{k}, \mathbf{q}} \hbar \sigma_{\mu, \nu}^{\mathbf{k}, \mathbf{k}'}(q_z) g_{\alpha, \mathbf{q}}^\mu a_{\mu, \mathbf{k}+\mathbf{q}}^\dagger a_{\mu, \mathbf{k}} (b_{\alpha, \mathbf{q}} + b_{\alpha, -\mathbf{q}}^\dagger) \quad (8)$$

is the electron-phonon interaction with the confinement factor

$$\sigma_{\mu, \nu}^{\mathbf{k}, \mathbf{k}'}(q_z) = \int dz \zeta_{\mu, \mathbf{k}}(z)^* \zeta_{\nu, \mathbf{k}'}(z) e^{iq_z z}. \quad (9)$$

In polar crystals (e.g., GaAs), the dominant electron-phonon coupling is given by the Fröhlich-interaction. By contrast, in nonpolar crystals as considered here (e.g., Si, Ge), the interaction is dominated by the optical deformation potential. We distinguish between the phonon-matrix element $g_{\mathbf{q}}^\mu$ for the valence and conduction band. In order to keep the problem manageable we neglect the dispersion of the optical phonons $\Omega_{LO}(\mathbf{q}) = \Omega_{LO}$ and the angular dependence of the interaction matrix element

$$|g_{\mathbf{q}}^\mu| = |g^\mu| = \sqrt{\frac{M_1 + M_2}{4\rho L^3 \hbar \Omega_{LO} M_1 M_2}} \frac{|d_{opt}^\mu|}{a_0}, \quad (10)$$

with the atomic masses M_i , the mass density ρ , the optical deformation potential constant d_{opt}^μ , and the lattice constant a_0 .

Based on this Hamiltonian, we calculate the equation of motion for the interband polarization $P_{\mu\nu, \mathbf{k}} = \langle a_{\mu, \mathbf{k}}^\dagger a_{\nu, \mathbf{k}} \rangle$ which leads to the semiconductor-Bloch equations.¹⁶ The absorption can be calculated from the macroscopic polarization

$$P = \sum_{\nu \neq \mu, \mathbf{k}} P_{\mu\nu, \mathbf{k}}. \quad (11)$$

For the following discussion, we assume a two-band model where c denotes the energetically lowest conduction subband and v the energetically highest valence subband. The subband indices and confinement factors will be omitted in the following. For the dephasing of the polarization we use the relaxation-time approximation which leads to Lorentzian absorption tails on the low energy side. The correlation terms in the equation of motion for the microscopic polarization caused by the electron-phonon interaction

$$\left. \frac{\partial}{\partial t} P_{\mathbf{k}} \right|_{ph, corr} = i \sum_{\mathbf{q}} g_{\mathbf{q}}^v (F_{cv, \mathbf{k}, \mathbf{q}}^+ + F_{cv, \mathbf{k}, \mathbf{q}}^-) - i \sum_{\mathbf{q}} g_{\mathbf{q}}^c (G_{cv, \mathbf{k}, \mathbf{q}}^+ + G_{cv, \mathbf{k}, \mathbf{q}}^-), \quad (12)$$

couple to the phonon-assisted polarizations $F_{cv, \mathbf{k}, \mathbf{q}}^- = \langle a_{v, \mathbf{k}+\mathbf{q}}^\dagger a_{c, \mathbf{k}} b_{\mathbf{q}} \rangle$, $F_{cv, \mathbf{k}, \mathbf{q}}^+ = \langle a_{v, \mathbf{k}+\mathbf{q}}^\dagger a_{c, \mathbf{k}} b_{-\mathbf{q}}^\dagger \rangle$, $G_{cv, \mathbf{k}, \mathbf{q}}^- = \langle a_{v, \mathbf{k}}^\dagger a_{c, \mathbf{k}-\mathbf{q}} b_{\mathbf{q}} \rangle$, and $G_{cv, \mathbf{k}, \mathbf{q}}^+ = \langle a_{v, \mathbf{k}}^\dagger a_{c, \mathbf{k}-\mathbf{q}} b_{-\mathbf{q}}^\dagger \rangle$. In order to describe the direct transitions in a semiconductor it is sufficient to treat the electron-phonon interaction as a Markovian process. Using the Born-Markov approximation for both scattering terms—the electron-electron and the electron-phonon interaction—one obtains a consistent set of equations to describe direct semiconductor materials.¹⁶

In contrast to the direct transitions, where the electron-phonon interaction induces a dephasing of the interband polarization and a renormalization of the transition energies, we take memory effects for the indirect transitions into account. Thus, we have to derive the phonon-assisted polarization without Born-Markov approximation, obtaining four types of equations for the phonon-assisted quantities $F_{ij, \mathbf{k}, \mathbf{q}}^\pm$ and $G_{ij, \mathbf{k}, \mathbf{q}}^\pm$ where $i, j = c, v$. For $i = j$, $F_{ii, \mathbf{k}, \mathbf{q}}^\pm$ denotes a phonon-assisted density and for $i \neq j$, $F_{ij, \mathbf{k}, \mathbf{q}}^\pm$ denotes a phonon-

assisted polarization. Here, we exemplarily discuss the time evolution of the phonon-assisted polarizations $F_{cv,\mathbf{k},\mathbf{q}}^-$. The equations of motion for the other three terms follow analogously. The electron-electron interaction is treated on the Hartree-Fock level. We introduce the hole density $n_{h,\mathbf{k}}$ which is given by the absence of electrons in the valence band: $n_{h,\mathbf{k}}=1-n_{v,\mathbf{k}}$. The equation of motion of the phonon-assisted polarizations then follows as

$$\frac{d}{dt}F_{cv,\mathbf{k},\mathbf{q}}^- = -\frac{i}{\hbar}(\epsilon_{c,\mathbf{k}} - \epsilon_{v,\mathbf{k}+\mathbf{q}} + \hbar\Omega_{LO})F_{cv,\mathbf{k},\mathbf{q}}^- \quad (13a)$$

$$- \frac{i}{\hbar}(\Omega_{\mathbf{k}+\mathbf{q}}F_{cc,\mathbf{k},\mathbf{q}}^- - \Omega_{\mathbf{k}}F_{vv,\mathbf{k},\mathbf{q}}^-) \quad (13b)$$

$$+ \frac{i}{\hbar}(1 - n_{h,\mathbf{k}+\mathbf{q}} - n_{e,\mathbf{k}}) \sum_{\mathbf{k}' \neq 0} V_{\mathbf{k}'} F_{cv,\mathbf{k}+\mathbf{k}',\mathbf{q}}^- \quad (13c)$$

$$+ \frac{i}{\hbar} \left(P_{\mathbf{k}+\mathbf{q}} \sum_{\mathbf{k}' \neq 0} V_{\mathbf{k}'} F_{cc,\mathbf{k}+\mathbf{k}',\mathbf{q}}^- - P_{\mathbf{k}} \sum_{\mathbf{k}' \neq 0} V_{\mathbf{k}'} F_{vv,\mathbf{k}+\mathbf{k}',\mathbf{q}}^- \right) \quad (13d)$$

$$+ \frac{i}{\hbar}(P_{\mathbf{k}} - P_{\mathbf{k}+\mathbf{q}})V_{\mathbf{q}} \sum_{\mathbf{k}'} (F_{vv,\mathbf{k}+\mathbf{k}',\mathbf{q}}^- + F_{cc,\mathbf{k}+\mathbf{k}',\mathbf{q}}^-) \quad (13e)$$

$$+ i(g_{\mathbf{q}}^v N_E(\mathbf{q})P_{\mathbf{k}} - g_{\mathbf{q}}^c (N_E(\mathbf{q}) + 1)P_{\mathbf{k}+\mathbf{q}}) \quad (13f)$$

$$+ i(g_{\mathbf{q}}^v (1 - n_{h,\mathbf{k}+\mathbf{q}})P_{\mathbf{k}} + g_{\mathbf{q}}^c n_{e,\mathbf{k}}P_{\mathbf{k}+\mathbf{q}}). \quad (13g)$$

In the first term on the right hand side of Eq. (13), $\epsilon_{i,\mathbf{k}}$ denotes the single-particle energies including the Coulomb renormalization. This term leads to oscillations with the frequency $\epsilon_{c,\mathbf{k}} - \epsilon_{v,\mathbf{k}+\mathbf{q}} + \hbar\Omega_{LO}$. Here, we include a phenomenological broadening by adding $-i\gamma$ to the frequency and choose γ in the range of some meV.

The second term describes the coupling of the system to the light-field with the renormalized Rabi-frequency

$$\Omega_{\mathbf{k}} = \mathcal{E}(t)d_{cv} + \sum_{\mathbf{k}' \neq 0} V_{\mathbf{k}'} P_{\mathbf{k}+\mathbf{k}'} \quad (14)$$

and the phonon-assisted density. These first two summands [Terms (13a) and (13b)] occur in complete analogy to terms in the semiconductor Bloch equations if one replaces the phonon-assisted polarizations and densities by the direct ones. The terms (13c)–(13e) are also renormalization terms caused by the Coulomb interaction. We assume that the carriers are in thermal equilibrium, so we can approximate the electron and hole densities ($n_{e,\mathbf{k}}$ and $n_{h,\mathbf{k}}$) by Fermi-functions. The light interaction term (13b) and Coulomb terms (13c)–(13e) are incompatible with the Markov approximation whereby we have to take memory effects into account.²⁴ The two last summands [Terms (13f) and (13g)] represent the source of the phonon-assisted polarization. The occupation of the phonons $N_E(\mathbf{q})$ is given by the Bose-Einstein distribution. In the derivation, we have neglected all higher-order scattering processes as, e.g., two-phonon scattering.

We conclude that phonon-assisted polarization can be generated in two ways.

(1) A finite phonon-assisted density couples to the classical light field [Term (13f)].

(2) Interband polarization seeds the phonon-assisted polarization [Term (13g)].

III. BAND STRUCTURE AND MODEL PARAMETER

We limit our discussion to a two-band model with an axially symmetric band structure ($\epsilon_{\mu,\mathbf{k}} = \epsilon_{\mu,|\mathbf{k}|} = \epsilon_{\mu,k}$) and assume spatial homogeneity ($n_{\mu,\mathbf{k}} = n_{\mu,|\mathbf{k}|} = n_{\mu,k}$). Hence, if we neglect the angular dependence of the phonon-matrix element $g_{\mathbf{q}}^{\mu} = g_{|\mathbf{q}|}^{\mu}$, the phonon-assisted polarization only depends on $|\mathbf{k}+\mathbf{q}|$, $F_{i,j,\mathbf{k},\mathbf{q}}^{\pm} = F_{i,j,k,q,\varphi}^{\pm}$, where φ represents the angle between the wave vectors \mathbf{k} and \mathbf{q} .

For the effective masses, we choose $m_e^* = 0.03m_0$ for the electrons at the boundary of the first Brillouin zone and $m_h^* = 4m_e^*$ for the holes at the Γ -Point, where m_0 is the electron mass. As we will see in Sec. IV, the indirect transitions depend either on the hole chemical potential or on the electron chemical potential. Thus we need high carrier concentrations at the end of the first Brillouin zone in order to obtain optical gain from the indirect transition, which depends on the electron chemical potential.

Figure 1(a) shows the band structure of our system. We assume parabolic bands with a maximum at the Γ point for the holes and with a minimum at the boundary of the first Brillouin zone for the electrons. Thus, electrons and holes are fully separated in momentum space. We consider gain and absorption in an energy interval around the indirect band gap $E_{g,ind}$, $E_{g,ind} - \hbar\Omega_{LO} < E < E_{g,ind} + \hbar\Omega_{LO}$. The direct transition does not fall into the interval and is thus not taken into account. Furthermore we restrict our discussion to the scattering processes where the momentum exchange is large enough for the carrier to recombine. All other scattering processes lead to a dephasing of the polarization which can be treated with a phenomenological dephasing time. Figure 1(b) shows the confinement potential and the confinement wave functions of our quantum well. We assume a strong confinement for the holes at the Γ point and a weak confinement for the electrons at the end of the first Brillouin zone.

Considering semiconductors crystallizing in diamond or zincblende structure, one can show that for symmetry reasons, the interaction between electrons in the conduction band and optical phonons is not allowed for the deformation potential interaction, $d_{opt}^{cb} = 0$ (Ref. 25). Thus, the intervalley scattering process is the only possible interaction between conduction band electrons and phonons.²⁶ In silicon the intervalley scattering between the Γ and the L valley or the Γ and X valley is not allowed,²⁷ only the L - L , X - X , and X - L scattering is allowed. In our calculation, we consider only scattering processes between the center and the end of the first Brillouin-zone and thus neglect any interaction between conduction band electrons and phonons. The deformation potential constant for the valence band is set to $d_{opt}^{vb} = 40$ eV, which is typical for tetrahedrally coordinated semiconductors.²⁵

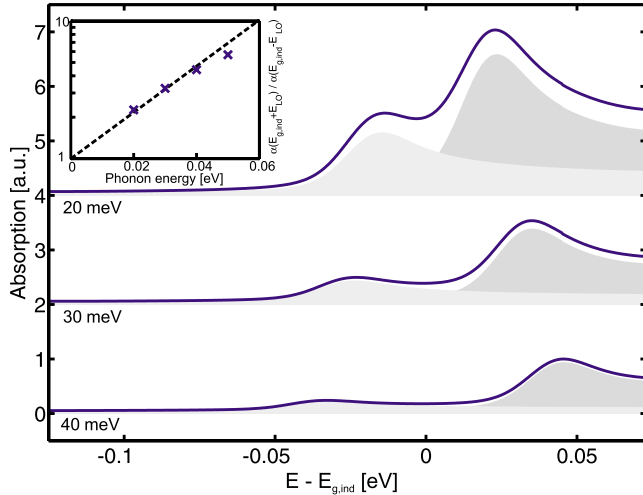


FIG. 2. (Color online) Absorption of a quantum well around the indirect band gap $E_{g,ind}$ in the low density limit for phonon energies $\hbar\Omega_{LO}=20, 30,$ and 40 meV at a carrier density of $d=10^8$ cm $^{-2}$. Inset: Ratio of the maximum absorption of the indirect transitions for different phonon energies on a logarithmic scale. The dashed line represents Eq. (15) and the crosses denote the microscopic calculation where we calculated both indirect transitions separately.

IV. RESULTS

A. Absorption of indirect semiconductors

The optical properties of direct semiconductors have been discussed in many publications (see e.g., Ref. 19). One important result is the fact that the maximum gain never exceeds the maximum absorption of the continuum states.

In this section, we discuss the low-density absorption of indirect semiconductors. We include a static Lindhard screening of the Coulomb potential. The numerical effort can dramatically be reduced by omitting the Coulomb renormalization terms (13c) and (13e). We checked both calculations and obtained only slight differences which are overcome by the higher resolution in the reciprocal space that we can use when omitting these Coulomb terms. Disorder effects are included by a 10 meV inhomogeneous broadening of the absorption spectra. Figure 2 shows the absorption spectrum of an indirect semiconductor around the indirect band gap $E_{g,ind}$ for phonon energies of $\hbar\Omega_{LO}=20, 30,$ and 40 meV. We obtain two unequally sized peaks around the phonon-assisted transitions $E_{g,ind} \pm \hbar\Omega_{LO}$. In all cases, the absorption of the transition at $E_{g,ind} + \hbar\Omega_{LO}$ is stronger than the absorption at $E_{g,ind} - \hbar\Omega_{LO}$. The absorption at $E_{g,ind} + \hbar\Omega_{LO}$ is the sum of the absorption of the energetically higher transition plus the absorption continuum of the energetically lower transition which is represented by the light and dark gray shaded areas in Fig. 2. Thus, the strength of both transitions can only be compared when calculating the absorption spectrum for both transitions separately by only taking $F_{cv,k,q}^-$ (dark gray) for the energetically higher transition and $F_{cv,k,q}^+$ (light gray) for the energetically lower transition in Eq. (12) into account.

The ratio of the maximal absorption of both transitions was calculated in a simple one-particle-model to be

$$\frac{\alpha(E_{g,ind} + \hbar\Omega_{LO})}{\alpha(E_{g,ind} - \hbar\Omega_{LO})} = \exp\left(\frac{\hbar\Omega_{LO}}{k_B T}\right), \quad (15)$$

where k_B is the Boltzmann factor and T the temperature.¹² Equation (15) was originally proposed for the ratio between the maximum optical gain at high-carrier densities and the maximum absorption in the case of zero carrier density, but this expression also holds for the ratio of the absorption of both transitions in the low density limit.¹² Since the situation for gain is more complicated because of different chemical potentials for the electrons and holes (see Sec. IV B), we use the expression in the low density limit. The inset of Fig. 2 shows the ratio of the maximum absorption of both indirect transitions for different phonon energies. Here, we calculated the absorption of the indirect transitions separately. The dashed line represents the result of Eq. (15) and the crosses denote the microscopic simulation with a carrier density $d = 10^8$ cm $^{-2}$. We obtain a good agreement between the microscopic calculation and the rate model. The difference between both calculations can be explained by looking at the conditions of Eq. (15). It holds exactly only for the case $\mu_e = \mu_h$ and $d=0$, where μ_e is the chemical potential of the electrons and μ_h is the chemical potential of the holes whereas we deal with a band structure where $\mu_e \neq \mu_h$ and consider finite carrier concentrations. Another reason is caused by the dephasing time approximation of the polarization which leads to a Lorentzian shaped tail of the absorption at the direct band edge. Thus, one obtains an unphysical absorption below the band gap, which vanishes very slowly for lower energies. Although the direct band gap is significantly higher than the indirect transitions its influence is still present. For numerical reasons, we have used a reduced direct band gap of 1.7 meV, further aggravating the effect which becomes stronger with increasing phonon energies.

B. Optical gain in indirect semiconductors

In this section, we discuss the influence of high carrier densities on the absorption spectrum of an indirect semiconductor. Figure 3 shows the absorption for carrier densities from $d=0.001 \times 10^{12}$ cm $^{-2}$ up to $d=9.0 \times 10^{12}$ cm $^{-2}$. For increasing densities, we obtain a red shift of both indirect transitions in the low- and high-density region. This is principally different to a direct semiconductor, where the absorption peak stays at a constant energy until at a certain density it starts blueshifting.¹⁶ Furthermore, in Fig. 3 the transparency density as well as the maximum optical gain differ between transitions. At the energetically lower transition one obtains optical gain for smaller carrier concentrations and reaches a higher maximum gain than for the energetically higher one.

Comparing both indirect transitions at equal carrier densities, we obtain a saturation of the energetically higher transition for densities up to $d=9.0 \times 10^{12}$ cm $^{-2}$, but still an increase in the gain of the energetically lower transition. This results from the fact that the source term of the phonon-assisted polarization $F_{cv,k,q}^-$ given by Eq. (13)—which represents the energetically higher transition—depends only on the hole distribution whereas the source term of $F_{cv,k,q}^+$,

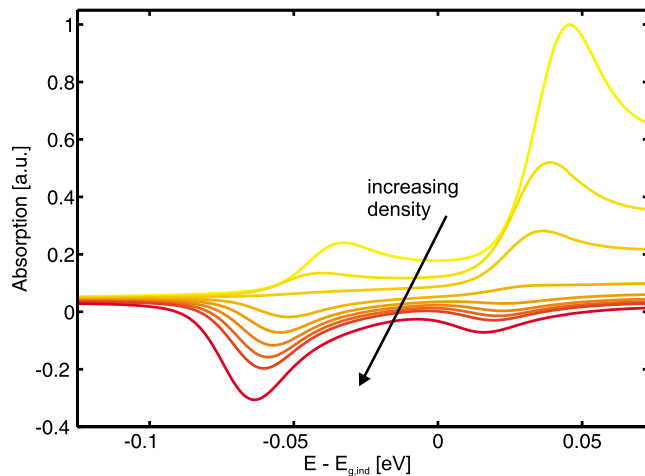


FIG. 3. (Color online) Absorption of an indirect semiconductor quantum well at carrier densities $d=0.001, 0.5, 1.0, 2.0, 3.0, 4.0, 5.0, 6.0,$ and $9.0 \times 10^{12} \text{ cm}^{-2}$.

which represents the energetically lower transition depends only on the electron distribution because of the optical deformation potential in the conduction band $\mu_{opt}^c=0$. Thereby the energetically higher transition depends on the hole density at the Γ point, more precisely the hole chemical potential, and the lower transition is controlled by the electron chemical potential.

In Fig. 4, the maximum absorption or gain of the indirect transition is plotted against the corresponding chemical potential. The triangles represent the microscopic calculation and the dashed line represents the rate model.¹² We now obtain a similar behavior for both transitions. The absorption and the gain saturate at equal chemical potentials. The maximum gain which can be reached by the energetically lower transition is higher than its maximum absorption. This asymmetric behavior which was already proposed earlier¹² can, thus, be reproduced by our microscopic many-body calculation. As mentioned in the previous section, the Lorentzian tail of the direct transition overlaps with the indirect transitions. Thus, the absorption is increased and the gain reduced by the relaxation time approximation.

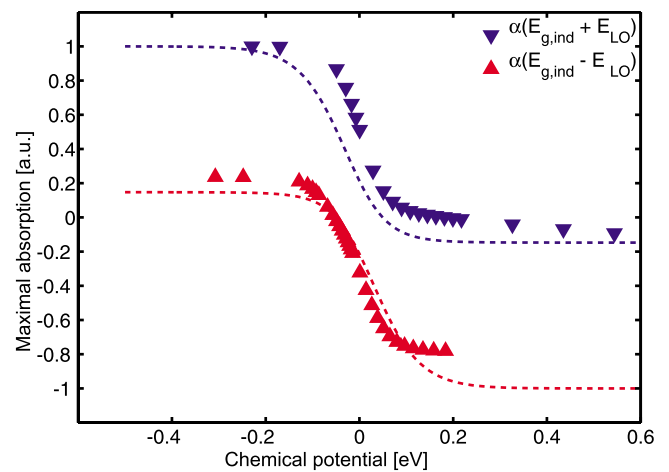


FIG. 4. (Color online) Maximum absorption of both transitions as a function of the chemical potential. Upper curve: Absorption around $E_{g,ind} + \hbar\Omega_{LO}$ for different hole chemical potentials μ_h . Lower curve: Absorption around $E_{g,ind} - \hbar\Omega_{LO}$ for different electron chemical potentials μ_e . Triangles represent the microscopic calculation and dashed lines are results obtained by a simple rate model (Ref. 12).

V. CONCLUSIONS

We have presented a microscopic theory for the interband transitions in indirect semiconductors. The optical properties of the indirect transitions differ strongly from those of a direct semiconductor. We show that the optical gain has an asymmetric behavior for different carrier densities. Furthermore the maximum optical gain can exceed the maximum absorption by orders of magnitude, which is completely different from the case of a direct semiconductor. In contrast to a previous simple one-particle model,¹² realistic band structure parameters enter our calculation. We thus have to deal with different electron and hole distributions because of their specific effective masses and number of Γ and L valleys. The different electron and hole chemical potentials are directly mirrored in the absorption or gain, where the indirect transition accompanied by the creation of a phonon depends on the hole chemical potential and the transition accompanied by the annihilation of a phonon depends on the electron chemical potential.

*sebastian.imhof@physik.tu-chemnitz.de

¹B. Kunert, K. Volz, J. Koch, and W. Stolz, *Appl. Phys. Lett.* **88**, 182108 (2006).

²A. J. Steckl, J. H. Park, and J. M. Zavada, *Mater. Today* **10**, 20 (2007).

³A. W. Fang, H. Park, Y. hao Kuo, R. Jones, O. Cohen, D. Liang, O. Raday, M. N. Sysak, M. J. Paniccia, and J. E. Bowers, *Mater. Today* **10**, 28 (2007).

⁴G. Roelkens *et al.*, *Mater. Today* **10**, 36 (2007).

⁵A. G. Cullis and L. T. Canham, *Nature (London)* **353**, 335 (1991).

⁶B. Gelozz, A. Kojima, and N. Koshida, *Appl. Phys. Lett.* **87**, 031107 (2005).

⁷Z. H. Lu, D. J. Lockwood, and J.-M. Baribeau, *Nature (London)* **378**, 258 (1995).

⁸G. Davies, *J. Lumin.* **80**, 1 (1998).

⁹T. Trupke, J. Zhao, A. Wang, R. Corkish, and M. A. Green, *Appl. Phys. Lett.* **82**, 2996 (2003).

¹⁰C.-Y. Tsai, *J. Appl. Phys.* **99**, 053506 (2006).

¹¹M. J. Chen, C. S. Tsai, and M. K. Wu, *Jpn. J. Appl. Phys.* **45**, 6576 (2006).

¹²T. Trupke, M. A. Green, and P. Würfel, *J. Appl. Phys.* **93**, 9058 (2003).

¹³H. Haug, *J. Appl. Phys.* **39**, 4687 (1968).

¹⁴H. Haug and S. Koch, *Phys. Status Solidi B* **82**, 531 (1977).

¹⁵O. Madelung, *Semiconductors-Basic Data*, 2nd ed. (Springer-

- Verlag, Berlin/Heidelberg/New York, 1996).
- ¹⁶H. Haug and S. W. Koch, *Quantum Theory of the Optical and Electronic Properties of Semiconductors*, 5th ed. (World Scientific, Singapore, 2009).
- ¹⁷A. Thränhardt, H. J. Kolbe, J. Hader, T. Meier, G. Weiser, and S. W. Koch, *Appl. Phys. Lett.* **73**, 2612 (1998).
- ¹⁸C. Schlichenmaier *et al.*, *Appl. Phys. Lett.* **86**, 081903 (2005).
- ¹⁹C. Bückers, S. Imhof, A. Thränhardt, J. Hader, J. V. Moloney, and S. W. Koch, *IEEE J. Sel. Top. Quantum Electron.* **15**, 984 (2009).
- ²⁰H. C. Schneider, W. W. Chow, and S. W. Koch, *Phys. Rev. B* **70**, 235308 (2004).
- ²¹F. Milde, A. Knorr, and S. Hughes, *Phys. Rev. B* **78**, 035330 (2008).
- ²²A. Grodecka-Grad and J. Förstner, *Phys. Rev. B* **81**, 115305 (2010).
- ²³W. Pötz and P. Vogl, *Phys. Rev. B* **24**, 2025 (1981).
- ²⁴C. N. Böttge, Diploma thesis, Philipps-Universität Marburg, 2009.
- ²⁵P. Y. Yu and M. Cardona, *Fundamentals of Semiconductors*, 1st ed. (Springer-Verlag, Berlin/Heidelberg/New York, 1996).
- ²⁶C. Jacoboni and L. Reggiani, *Rev. Mod. Phys.* **55**, 645 (1983).
- ²⁷M. Fischetti, *IEEE Trans. Electron Devices* **38**, 634 (1991).